INŽENÝRSKÁ MECHANIKA 2005
NÁRODNÍ KONFERENCE
s mezinárodní účastí
Svratka, Česká republika, 9. - 12. května 2005

A NOVEL QUANTITATIVE DESCRIPTION OF ELECTROPHYSIOLOGICAL PROCESSES IN GUINEA PIG VENTRICULAR CARDIOMYOCYTES

M. Pásek[1], G. Christé[2], J. Šimurda[3]

Summary: *A novel quantitative model of a guin ea-pig ventricular myocyte has been designed with transverse-axial tubular system (TATS) included. This model displays long-term stability and closely reproduces experimental activity-related changes in action potentials and io nic concentrations inside the cell and in the lumen of the TATS. It allows e xploration of species-specific functional consequences of the presence of the TATS in a biophysically realistic way.*

1. Introduction

In our previous work (Pásek et al., 2001; 2002; 2003) we developed a generic model of cardiac ventricular cell electrical activity incorporating a quantitative description of the transverse-axial tubular system (TATS). The later stage of our work was focused on design of models related to specific species, namely rat and guinea pig. The model of rat ventricular cell was published in Pásek et al. (2004). In this work, we describe a novel model of guinea pig ventricular cardiomyocyte that is intended for exploration of specific electrophysiological processes related to function of TATS in guinea pig heart.

2. Formulation of the model

The formulation of the model is biophysically consistent with other models of guinea pig ventricular cell published so far (Nordin, 1993; Noble et al., 1998; Faber and Rudy, 2000). However our model differs in two significant ways. Firstly, a compartment representing the TATS was incorporated. Secondly, new equations describing original experimental data from the guinea pig were formulated and incorporated, where available. The restricted ion diffusion between tubular and extracellular space was included. The formulation of intracellular Ca^{2+} handling includes a restricted subsarcolemmal compartment ('dyadic space'), uptake and release compartment of sarcoplasmic reticulum and Ca^{2+} buffers. A schematic diagram of the model is shown in Fig. 1.

[1] Ing. Michal Pásek, Ph.D.: Institute of Thermomechanics, Czech Academy of Science - branch Brno; Technická 2; 616 69 Brno; Czech Republic; e-mail: pasek@umtn.fme.vutbr.cz
[2] Dr. Georges Christé.: INSERM E0219, DRDC/DVE, CENG F-38054, Grenoble; CEDEX 9; France
[3] Doc. RNDr. Jiří Šimurda CSc.: Institute of Physiology of Masaryk University, Komenského nám. 2; Brno; Czech Republic

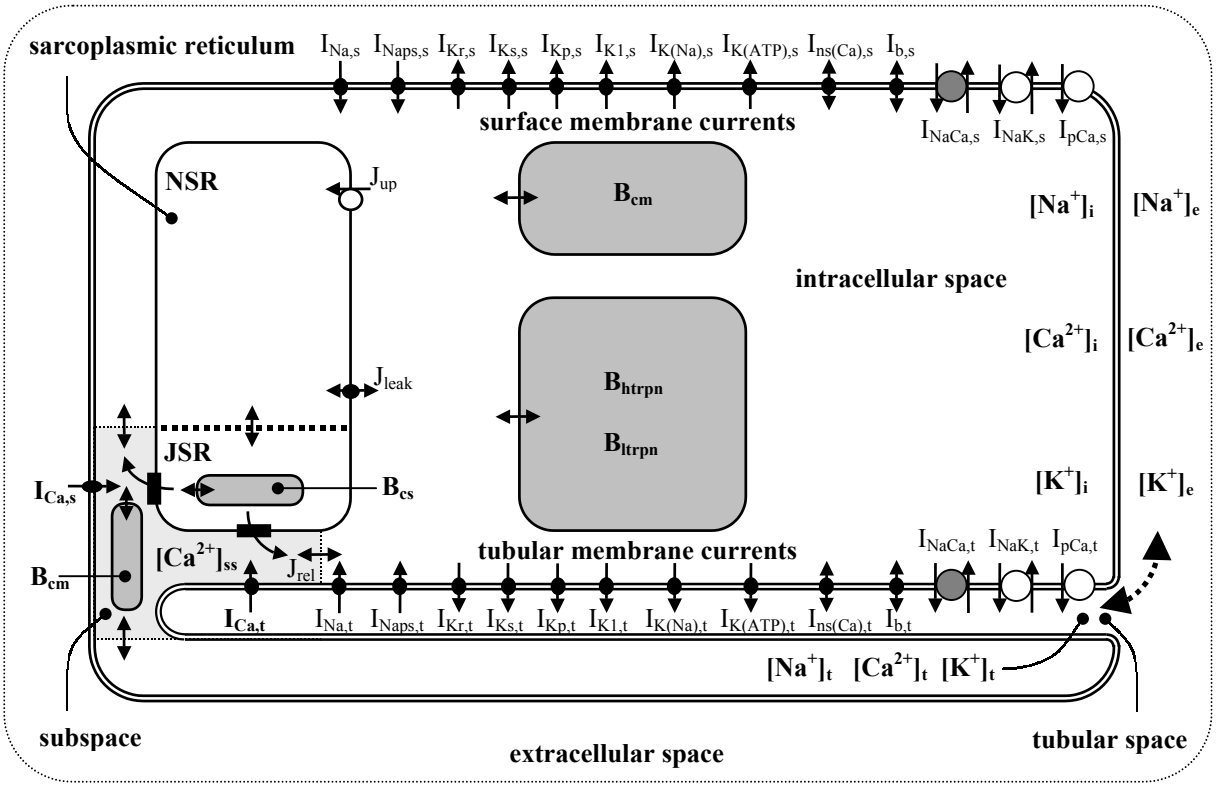

Figure 1. Schematic diagram of the ventricular cell model. The description of electrical activity of surface (s) and tubular (t) membrane comprises formulation of the following ion currents: fast sodium current (I_{Na}), persistent sodium current (I_{Naps}), calcium currents through L-type channels (I_{Ca}), fast and slow component of delayed rectifier potassium currents (I_{Ks}, I_{Kr}), plateau potassium current (I_{Kp}), inward rectifying potassium current (I_{K1}), Na^+ sensitive potassium current ($I_{K(Na)}$), ATP sensitive potassium current ($I_{K(ATP)}$), non-specific calcium-activated current ($I_{ns(Ca)}$), background calcium current (I_{Cab}), background sodium current (I_{Nab}), sodium-calcium exchange current (I_{NaCa}), sodium-potassium pump current (I_{NaK}) and calcium pump current (I_{pCa}). The intracellular space contains the subspace, the Ca^{2+}-uptake and Ca^{2+}-release compartments of sarcoplasmic reticulum (NSR, JSR) and the Ca^{2+} buffers calmodulin (B_{cm}), troponin (B_{htrpn}, B_{ltrpn}) and calsequestrin (B_{cs}). The small filled rectangles in JSR membrane represent ryanodine receptors. The small bi-directional arrows denote Ca^{2+} diffusion. Ionic diffusion between the tubular and the bulk space is represented by the dashed arrow.

Geometric parameters of the cell and of the TATS

The dimensions of the guinea pig ventricular myocyte have been measured by several groups (Shepherd and McDonough, 1998; Wang et al., 1997, Amsellem et al., 1995). On the basis of these data, the shape of the cell in the model is represented as a cylinder 130 μm in length and 12 μm in diameter. The volume fractions of intracellular compartments: myoplasm (68 %), sarcoplasmic reticulum (5.5 % JSR and 0.32 % NSR), and dyadic-space (0.00041 %) are those proposed by Jafri et al. (1998).

The geometric parameters of the TATS were set to comply with the results of microscopic analysis of guinea pig ventricular myocytes (Amsellem et al, 1995): fractional volume 2.9 %,

fractional area 52.6 %, surface/volume ratio 13.5 μm^2 μm^{-3}. Applying these parameters in the model and assuming the mean length of tubules (l_t) to be comparable to cellular radius (6 μm), the tubular membrane represents 5.62 10^{-5} cm^2 (56.2 pF) and the peripheral membrane represents 5.06 10^{-5} cm^2 (50.6 pF).

Distribution of ionic currents among peripheral and tubular membranes

The fractions of individual ionic currents in the TATS were set using data mainly obtained from measurements on guinea pig ventricular cardiomyocytes.

I_{Na} - the fast Na^+ current in guinea-pig cells was reported to be preferentially distributed in the TATS as followed from the analysis of the slow of decrease of I_{Na} upon reduction of Na^+ ions in the extracellular medium (Shepherd and McDonough, 1998). However, to attain the best fit with their experimental data we assigned 53 % of this current to the tubular membrane in the model.

I_{Ca} - the Ca^{2+} current through L-type Ca^{2+} channels is generally associated with ryanodine receptors at the dyads, which occur predominantly at the TATS (Scriven et al., 2000; Brette and Orchard, 2003). This is consistent with the 64 % of I_{Ca} being restored with a slow time course after Ca^{2+} repletion in the extracellular medium (Shepherd and McDonough, 1998). On the basis of these results we assigned 64 % of this current to the tubular membrane, which was justified by the model simulations.

I_{Kr} and ***I_{Ks}*** - the rapid and slow components of delayed rectifier K^+ current have also been reported to be preferentially located at the TATS membrane (Rasmussen et al., 2004). However, as a sizeable part of the immunolabeling of ERG appeared near the mouth of the tubules (Rasmussen et al., 2004), where it would neither be contributing nor be sensing any significant accumulation-depletion of K^+, we assumed these channels to be uniformly distributed between the tubular and surface membranes.

I_{K1} - 83 % of the inward rectifying K^+ current appears to be lost when rabbit cells lose their TATS; furthermore, the time course of onset of the block by barium ions shows a sigmoid onset suggesting the presence of a diffusion delay (Christé, 1999). Immunocytochemical studies by Christé et al. (unpublished) and by Clark et al. (2001) also support this view. 80 % of this current was thus assigned to the tubular membrane.

I_{NaCa} - the Na^+-Ca^{2+} exchange current was reported to be mainly located in TATS of guinea pig (Frank et al. 1992). However, Kieval et al. (1992) reported a more even distribution in rat and guinea pig cells. We assumed a 70 % fraction of this current to be in tubular membrane.

I_{NaK} - the Na^+-K^+ pump protein immunolabeling was found to be distributed uniformly in guinea pig cells (McDonough et al. 1996). The fraction of I_{NaK} in tubular membrane was therefore set to 52.6 %.

I_{pCa} - the Ca^{2+} pump current and its localization in cellular membrane of guinea pig was studied by Iwata et al. (1994). They found immunofixation of anti Ca^{2+}-pump antibodies to predominate at the surface membrane and to be scarce within the TATS, thus a 20 % fraction of I_{pCa} in tubular membrane was assumed.

$I_{K(ATP)}$ - the ATP sensitive K^+ current. A tail current could be recorded in guinea-pig cells following activation of the ATP sensitive K^+ current ($I_{K,ATP}$) (Yasui et al., 1993; Tourneur et al., 1994) meaning that K_{ATP} channels are present in the TATS and cause K^+ accumulation.

We observed the presence of dense labeling of transverse tubules by antibody against Kir6.2 channel subunit in rabbit ventricular cardiomyocytes (Christé et al., unpublished). Korchev et al. (2000) recorded maximal K^+ current density around the mouths of T-tubules by high-resolution scanning patch clamp. This could mean that part of the K_{ATP} channels are not within the TATS. As quantitative estimation of the distribution of K_{ATP} channels is still missing, we set uniform density to the K_{ATP} channels in the model resulting in 52.6 % fraction of $I_{K,ATP}$ in tubular membrane.

Data are unavailable for the distribution of the persistent Na^+ current (I_{Naps}), the plateau K^+ current (I_{Kp}), the non-specific Ca^{2+}-activated current (I_{nsCa}) and background currents ($I_{Na,b}$, $I_{Ca,b}$), so their distribution was assumed to be uniform (52.6 % fraction in TATS) over the whole cellular membrane.

The numerical values of the fractions of individual ion currents in the TATS are listed in Table 1, together with the magnitude of maximum current, conductivity or permeability of related transporters in peripheral and tubular membrane.

Table 1. Electrical properties of surface and tubular membrane transport systems used in the model. The transport systems are listed in the first column. The second column shows values of the whole cell maximum conductivities (g), permeabilities (P) or currents (I_{max}) related to individual transporters. The two next columns indicate the same parameters related to surface and peripheral membrane, respectively. The units are specified in the fourth column. The last column shows the fractions of ion transporters in the TATS as obtained from literature. When no data could be found, the densities of ion transfer mechanisms were assumed to be equally distributed between both membrane systems. The values denoted by asterisks hold for the following concentrations: $[K^+]_e = 5.4$ mM, $[Ca^{2+}]_i = 37.52$ nM and $[ATP]_i = 6.8$ mM.

parameter	total membrane	surface membrane	tubular membrane	unit	fraction in TATS
g_{Na}	30	22.79	36.495	[mS cm^{-2}]	0.64 %
g_{Naps}	0.0053	0.0053	0.0053	[mS cm^{-2}]	0.526 %
g_{Kr}	0.0209*	0.0209*	0.0209*	[mS cm^{-2}]	0.526 %
g_{Ks}	0.1075*	0.1075*	0.1075*	[mS cm^{-2}]	0.526 %
g_{K1}	0.75*	0.3165*	1.1405*	[mS/cm^{-2}]	0.8 %
g_{Kp}	0.006	0.006	0.006	[mS cm^{-2}]	0.526 %
$g_{K(Na)}$	0.1285	0.1285	0.1285	[mS cm^{-2}]	0.526 %
$g_{K(ATP)}$	0.0003*	0.0003*	0.0003*	[mS cm^{-2}]	0.526 %
$g_{Na,b}$	0.0007	0.0007	0.0007	[mS/cm^{-2}]	0.526 %
$g_{Ca,b}$	0.0021	0.0021	0.0021	[mS/cm^{-2}]	0.526 %
$P_{Ca,L}$	0.0048	0.0036	0.0058	[cm s^{-1}]	0.64 %
$P_{K,L}$	4.80E-6	3.65E-6	5.84E-6	[cm s^{-1}]	0.64 %
$P_{ns(Na)}$	1.75E-7	1.75E-7	1.75E-7	[cm s^{-1}]	0.526 %
$P_{ns(Ca)}$	1.75E-7	1.75E-7	1.75E-7	[cm s^{-1}]	0.526 %
$I_{pCa,max}$	1.15	1.9413	0.4372	[μA cm^{-2}]	0.2
$I_{NaK,max}$	1.5	1.5	1.5	[μA cm^{-2}]	0.526
k_{NaCa}	0.00025	0.00016	0.00033	[μA cm^{-2} mM^{-4}]	0.7

Description of voltage and time-dependent properties of ion transfer mechanisms

As there is no evidence that the properties of the ion transfer mechanisms are different in the tubular and peripheral membranes the ionic currents in both these subsystems were described by the same set of algebraic and differential equations. The currents I_{K1}, $I_{K(Na)}$, $I_{K(ATP)}$, $I_{ns(Ca)}$, I_{Nab}, I_{Cab}, I_{NaCa}, I_{NaK} and I_{pCa} were adopted from the model published by Faber and Rudy (2000) that is available in http://www.cwru.edu/med/CBRTC. The formulations of other currents (I_{Na}, I_{Naps}, I_{Ca}, I_{Kr}, I_{Ks} and I_{Kp}) are explained in the following section and their full description is introduced in appendix.

***I_{Na}*:** The classical Hodgkin-Huxley formalism with three activation (m^3) and one inactivation (h) gates is used to describe the function of guinea pig I_{Na}-channel. The voltage dependencies of steady state activation ($\overline{m}$), steady state inactivation ($\overline{h}$) and of related time constants (τ_m, τ_h) were derived from the experimental data of Li et al. (2002) obtained at 16 °C. The experimental and simulated currents are compared in Fig 2 A-D.

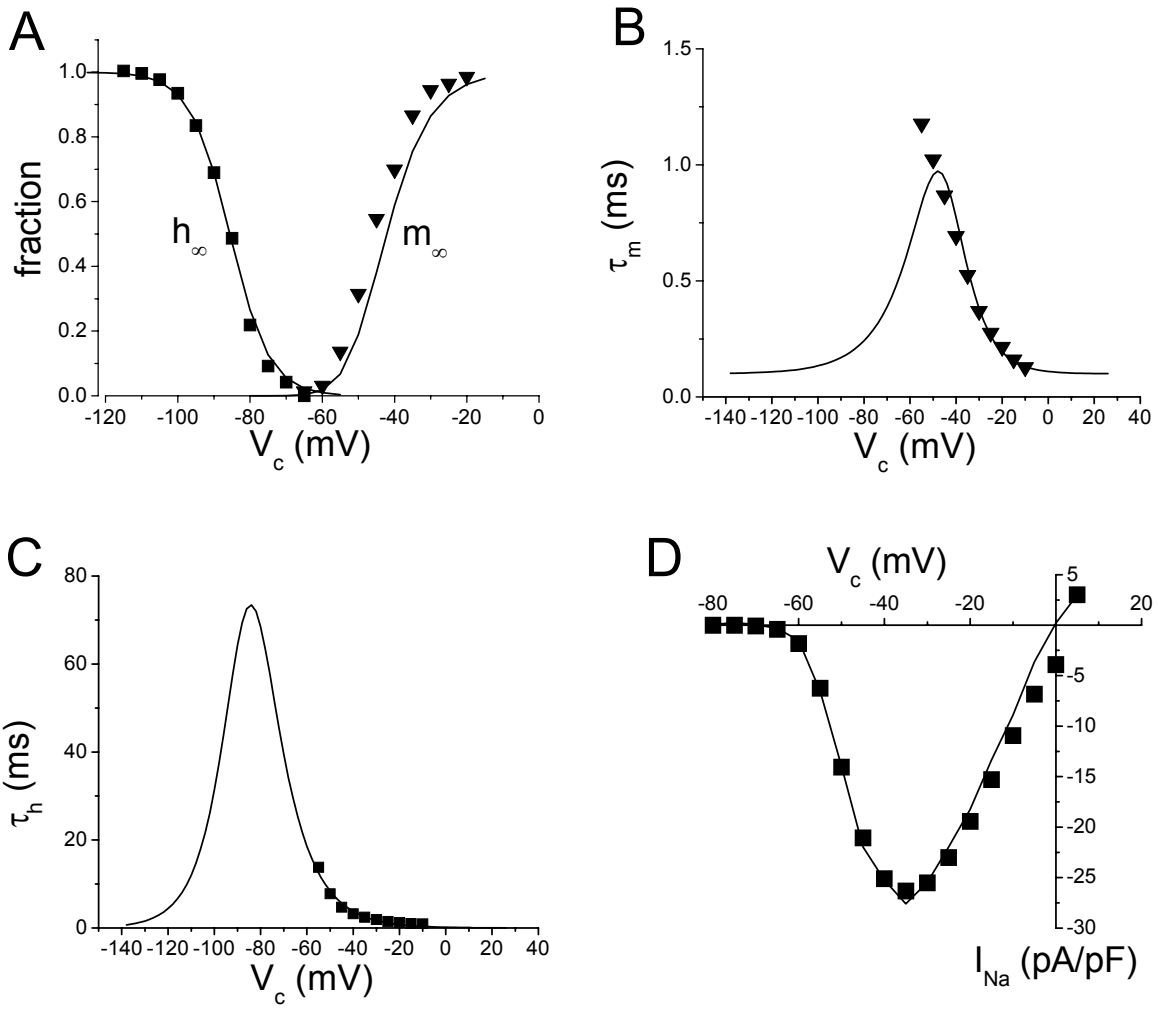

Figure 2: The comparison of data generated by the model before correction for 37 °C (solid lines) with the experimental data (filled squares or filled triangles) of Li et al. (2002). A) Voltage dependence of steady state activation (m_∞) and inactivation (h_∞). B) Voltage dependence of the time constant of activation: C) Voltage dependence of the time constant of inactivation. D) Peak I_{Na} versus command voltage (V_c).

To simulate the behaviour of I_{Na} at 37 °C the voltage dependence of m_∞ and h_∞ were shifted by 9 mV in positive direction (Nagatomo et al., 1998) and the rate of channel gating was increased by factor 4.83 (Colatsky, 1980; Nagatomo et al., 1998). The reversal potential (E_{Na}) was decreased by introduction a 12 % fractional permeability of the channel for K^+ ions (Nordin, 1993). The maximum channel conductance ($\overline{g}_{Na}$) was set to 30 mS μF^{-1} to generate the maximum upstroke velocity $(dV/dt)_{max}$ = 512 V s^{-1} as observed by Taniguchi et al. (1994) in single guinea pig cardiomyocytes.

I_{Naps}: There is recent evidence that, in addition to the TTX-sensitive Na^+ current and background Na^+ current, a tetrodotoxin-insensitive persistent sodium current (Sakmann et al. 2000) exists in guinea pig ventricular cells. This current was implemented using the description of Sakmann et al. (2000) and the parameters comprising the voltage at half-maximal activation (-54 mV), the slope factor (8 mV) and the maximum channel conductance (0.0053 mS μF^{-1}) were adjusted for the best fit with their experimental results. To account for the experimentally observed value of 33.5 mV for the reversal potential of I_{Nap} (E_{Nap}) we supplemented its formulation with 12 % fractional permeability for K^+ in the same way as in I_{Na} formulation.

$I_{Ca,L}$: The function of $I_{Ca,L}$-channels is described by the multi-state model designed by Jafri et al. (1998) for small mammals like guinea pig. The voltage dependence of steady-state inactivation was, however, modified to exhibit a sigmoid relationship (Findlay, 2002) and proper shape of action potentials (Wang et al., 1988; Grantham and Cannell, 1996). The channel permeability was lowered to 0.0048 cm s^{-1} (as compared with 0.0054 cm s^{-1} proposed by Jafri et al., 1998) to prevent intracellular Ca^{2+} overload at high frequencies of stimulation.

I_{Kr} and I_{Ks}: The formulation of I_{Kr} incorporates both the time-dependent activation gate and time-independent inactivation gate to approximate the very fast inactivation process of this channel. In contrast, the formulation of I_{Ks} is provided by two time dependent activation gates and does not include inactivation. Both current formulations are the same as described by Zeng et al. (1995) on the basis of experimental data from guinea pig cardiomyocytes (Sanguinetti and Jurkiewicz, 1990). The conductivities $g_{Kr([K]e=5.4\ mM)}$ = 0.0209 mS cm^{-2} and $g_{Ks([Ca]i=37.5\ nM)}$ = 0.456 mS cm^{-2} were adjusted to ensure a realistic duration of action potentials observed in guinea pig at 36 - 37 °C (Wang et al., 1998).

I_{Kp}: The formulation of the plateau potassium current I_{Kp} is based on the description used by Faber and Rudy (2000) but the voltage dependence of this current was modified to produce a plateau phase characteristic for guinea pig AP: the voltage for half activation was shifted to more positive voltages (from 7.5 mV to 20 mV) and the slope factor was decreased from 6 to 5.

$I_{ns(Ca)}$: The non-specific Ca^{2+}- activated current was included into the model to be able to simulate the arrhythmogenic behaviour under conditions of Ca^{2+} - overload. The formulation of ***$I_{ns(Ca)}$*** is the same as proposed by Faber and Rudy (2000) except for the half-saturation concentration in the term of Ca^{2+} - dependent activation. This was increased from 1.2 $mM.l^{-1}$ to 2.5 $mM.l^{-1}$ for ***$I_{ns(Ca)}$*** not to interfere with cellular electrical activity in physiological conditions.

To observe the charge conservation principle described by Hund et al. (2001) and ensure the long-term stability of the model, we incorporated the stimulus current (4.8 nA, 1 ms) into the equation controlling the intracellular potassium concentration.

Electrical interaction between surface and tubular membrane

The electrical interaction between surface and tubular membrane is formulated in the same way as previously described (Pásek et al. 2001).

Intracellular Ca^{2+} handling

The description of intracellular Ca^{2+} handling consists of formulations controlling the free Ca^{2+} concentrations in the dyadic space ($[Ca^{2+}]_{ss}$), intracellular space ($[Ca^{2+}]_i$) and sarcoplasmic reticulum compartments ($[Ca^{2+}]_{NSR}$, $[Ca^{2+}]_{JSR}$). The whole process including intracellular Ca^{2+} transport and intracellular Ca^{2+} buffering by troponin (B_{htrpn}, B_{ltrpn}), calmodulin (B_{cm}) and calsequestrin (B_{cs}) was adopted from the model by Jafri et al. (1998). Some parameters were, however, changed to simulate Ca^{2+} transients of guinea pig cardiomyocytes. The changes include: increase of Ca^{2+} maximum pump rate to 1.8 mM s^{-1}, increase of Ca^{2+} leak rate from the NSR into myoplasm to 0.0725 s^{-1} and increase of parameters (k_a^+, k_a^-) characterising rate of transition between P_{c1} and P_{o1} states of calcium release channel in JSR to 36.45×10^{12} mM^{-4} s^{-1} and 576 s^{-1}, respectively.

Ionic diffusion between tubular and extracellular space

The time constants of ion exchange between the TATS lumen and the bulk external solution ($\tau_{Na,t}$, $\tau_{Ca,t}$, $\tau_{K,t}$) were set for the model to reproduce closely changes in I_{Na}, I_{Ca} and holding current following rapid increase or decrease of external ion concentrations (Shepherd and McDonough, 1998). To reconstruct these experimental data, the model was supplemented by an external compartment describing fast ion exchange ($\tau_{Na,e}$, $\tau_{Ca,e}$, $\tau_{K,e}$) between the perfusion pipette and cellular surface. Using the same pulse and solution change protocol the reconstruction led to the following values of the constants: $\tau_{Na,e} = \tau_{K,e} = 22$ ms, $\tau_{Na,t} = \tau_{K,t} = 200$ ms, $\tau_{Ca,e} = 20$ ms, and $\tau_{Ca,t} = 240$ ms.

General conditions:

External bulk concentrations of Na^+, K^+ and Ca^{2+} ions were set constant to respectively $[Na^+]_e = 140$ mM, $[K^+]_e = 5.4$ mM and $[Ca^{2+}]_e = 1.8$ mM. Temperature was 37°C.

The basic units in which the equations were solved were: *mV* for membrane voltage, μA for membrane currents, *mmol* l^{-1} for ionic concentrations, *s* for time, and *ml* for volumes.

3. Conclusion

The present novel description of electrophysiological processes in guinea pig ventricular myocytes is based on previously published and validated models and includes improved formulations of some ionic currents according to recent experimental works. The main novelty lies, however, in addition of TATS that appears to play a significant role in modulation of electrophysiological processes in ventricular cardiomyocytes. Its morphology and physical characteristics are described to meet the data from ultra-structural studies of guinea pig myocytes. The resulting model shall be used for investigation of the effect of restricted ion diffusion in extracellular and intracellular space on cellular electrical activity and associated changes in intracellular ionic homeostasis.

4. Acknowledgments

This study was supported by the project AV0Z 20760514 from the Institute of Thermomechanics of Czech Academy of Sciences, partly by the project MSM 0021622402 from the Ministry of Education, Youth and Sports of the Czech Republic and by the Institut National de la Santé et de la Recherche Médicale (INSERM, France).

5. Appendix

The basic units in which the equations were solved were: *mV* for membrane voltage, μ*A* for membrane currents, *mmol l*$^{-1}$ for ionic concentrations, *s* for time, and *ml* for volumes. The suffix 'x' stands for 's' or 't' for surface and tubular currents, respectively, and the suffix 'o' stands for 'e' or 't' for extracellular or tubular ionic concentrations, respectively.

Na^+ current, I_{Na}

The underlined values in the description of I_{Na} are corrections introduced to adapt I_{Na} properties from 16°C to 37°C (see the main text).

$$I_{\mathrm{Na,x}} = g_{\mathrm{Na,x}} m_{\mathrm{x}}^{3} h_{\mathrm{x}} (V_{\mathrm{m,x}} - E_{\mathrm{Na,x}})$$

$$\frac{dm_{\mathrm{x}}}{dt} = \frac{\bar{m}_{\mathrm{x}} - m_{\mathrm{x}}}{\tau_{\mathrm{m,x}}}, \quad \frac{dh_{\mathrm{x}}}{dt} = \frac{\bar{h}_{\mathrm{x}} - h_{\mathrm{x}}}{\tau_{\mathrm{h,x}}}$$

$$\bar{m}_{\mathrm{x}} = \frac{1}{1 + e^{-(V_{\mathrm{m,x}} + 52.2 - \underline{9})/7.4}}$$

$$\bar{h}_{x} = \frac{1}{1 + e^{(V_{\mathrm{m,x}} + 85.6 - \underline{9})/5.5}}$$

$$\tau_{\mathrm{m,x}} = \underline{0.207}\left[\frac{0.001}{101.6e^{0.1135V_{\mathrm{m,x}}} + 0.02268e^{-0.0717*V_{\mathrm{m,x}}}} + 0.0001\right]$$

$$\tau_{\mathrm{h,x}} = \underline{0.207}\left[\frac{0.001}{1.1381\times10^{-6}\mathrm{e}^{-0.1017V_{\mathrm{m,x}}} + 6.537\mathrm{e}^{0.08016V_{\mathrm{m,x}}}} + 0.0005\right]$$

$$E_{\mathrm{Na,x}} = \frac{RT}{F}\frac{\left[\mathrm{Na}^{+}\right]_{\mathrm{o}} + 0.12\left[\mathrm{K}^{+}\right]_{\mathrm{o}}}{\left[\mathrm{Na}^{+}\right]_{\mathrm{i}} + 0.12\left[\mathrm{K}^{+}\right]_{\mathrm{i}}}$$

Persistent Na^+ current, I_{Naps}

$$I_{\mathrm{Naps,x}} = g_{\mathrm{Naps,x}} \frac{1}{1+\mathrm{e}^{-(V_{\mathrm{m,x}} + 54)/8}} (V_{\mathrm{m,x}} - E_{\mathrm{Na,x}})$$

L-type Ca^{2+} current, I_{Cal}

$$I_{\mathrm{CaL,x}} = P_{\mathrm{CaL,x}} (O_{\mathrm{x}} + O_{\mathrm{Ca,x}}) y_{\mathrm{x}} V_{\mathrm{m,x}} \frac{4F^2}{RT} \frac{0.001\mathrm{e}^{2V_{\mathrm{m,x}}F/(RT)} - 0.341\left[\mathrm{Ca}^{2+}\right]_{\mathrm{o}}}{\mathrm{e}^{2V_{\mathrm{m,x}}F/(RT)} - 1}$$

$$\frac{dC_{0,x}}{dt}=\beta_x C_{1,x}+\omega C_{Ca0,x}-(4\alpha_x+\gamma)C_{0,x}$$

$$\frac{dC_{1,x}}{dt}=4\alpha_x C_{0,x}-2\beta_x C_{2,x}+\frac{\omega}{b}C_{Ca1,x}-(\beta_x+3\alpha_x+\gamma a)C_{1,x}$$

$$\frac{dC_{2,x}}{dt}=3\alpha_x C_{1,x}+3\beta_x C_{3,x}+\frac{\omega}{b^2}C_{Ca2,x}-(2\beta_x+2\alpha_x+\gamma a^2)C_{2,x}$$

$$\frac{dC_{3,x}}{dt}=2\alpha_x C_{2,x}+4\beta_x C_{4,x}+\frac{\omega}{b^3}C_{Ca3,x}-(3\beta_x+\alpha_x+\gamma a^3)C_{3,x}$$

$$\frac{dC_{4,x}}{dt}=\alpha_x C_{3,x}+gO_x+\frac{\omega}{b^4}C_{Ca4,x}-(4\beta_x+f+\gamma a^4)C_{4,x}$$

$$\frac{dO_x}{dt}=fC_{4,x}-gO_x$$

$$\frac{dC_{Ca0,x}}{dt}=\beta'_x C_{Ca1,x}+\gamma C_{0,x}-(4\alpha'_x+\omega)C_{Ca0,x}$$

$$\frac{dC_{Ca1,x}}{dt}=4\alpha'_x C_{Ca0,x}+2\beta'_x C_{Ca2,x}+\gamma aC_{1,x}-(\beta'_x+3\alpha'_x+\frac{\omega}{b})C_{Ca1,x}$$

$$\frac{dC_{Ca2,x}}{dt}=3\alpha'_x C_{Ca1,x}+3\beta'_x C_{Ca3,x}+\gamma a^2 C_{2,x}-(2\beta'_x+2\alpha'_x+\frac{\omega}{b^2})C_{Ca2,x}$$

$$\frac{dC_{Ca3,x}}{dt}=2\alpha'_x C_{Ca2,x}+4\beta'_x C_{Ca4,x}+\gamma a^3 C_{3,x}-(3\beta'_x+\alpha'_x+\frac{\omega}{b^3})C_{Ca3,x}$$

$$\frac{dC_{Ca4,x}}{dt}=\alpha'_x C_{Ca3,x}+g'_x O_{Ca,x}+\gamma a^4 C_{4,x}-(4\beta'_x+f'+\frac{\omega}{b^4})C_{Ca4,x}$$

$$\frac{dO_{Ca,x}}{dt}=f'C_{Ca4,x}-g'O_{Ca,x}$$

$$\alpha_x=400e^{(Vm,x+12)/10}$$

$$\beta_x=50e^{-(Vm,x+12)/13}$$

$$\alpha'_x=a\alpha_x$$

$$\beta'_x=\frac{\beta_x}{b}$$

$$\gamma=187.5\left[Ca^{2+}\right]_{ss}$$

$$\frac{dy_x}{dt}=\frac{\bar{y}_x-y_x}{\tau_{y,x}}$$

$$\bar{y}_x=\frac{1}{1+e^{(V_{m,x}+35)/6}}$$

$$\tau_x=\frac{0.001}{0.02+0.0197e^{-((V_{m,x}+10)/29.67)^2}}+\frac{0.55}{1+e^{(V_{m,x}+40)/2.375}}$$

Rapid component of delayed rectifier K^+ current, I_{Kr}

$$I_{\mathrm{Kr,x}} = g_{\mathrm{Kr,x}}\sqrt{\frac{K_\mathrm{o}}{5.4}}x_{\mathrm{r1,x}}\bar{x}_{\mathrm{r2,x}}(V_{\mathrm{m,x}}\text{-}E_{\mathrm{K}})$$

$$\frac{dx_{\mathrm{r1,x}}}{dt} = \frac{\bar{x}_{\mathrm{r1,x}} - x_{\mathrm{r1,x}}}{\tau_{\mathrm{r1,x}}}$$

$$\bar{x}_{\mathrm{r1,x}} = \frac{1}{1+e^{\text{-}(\mathrm{V_{m,x}}+21.5)/7.5}}$$

$$\bar{x}_{\mathrm{r2,x}} = \frac{1}{1+e^{(\mathrm{V_{m,x}}+9)/22.4}}$$

$$\tau_{\mathrm{r1,x}} = \frac{1}{\dfrac{1.38(V_{\mathrm{m,x}}+14.2)}{1\text{-}e^{\text{-}(\mathrm{V_{m,x}}+14.2)/8.13}} - \dfrac{0.61(V_{\mathrm{m,x}}+38.9)}{1\text{-}e^{(\mathrm{V_{m,x}}+38.9)/6.89}}}$$

$$E_{\mathrm{K,x}} = \frac{RT}{F}\frac{\left[\mathrm{K}^+\right]_\mathrm{o}}{\left[\mathrm{K}^+\right]_\mathrm{i}}$$

Slow component of delayed rectifier K^+ current, I_{Ks}

$$\mathrm{I_{Ks,x}} = g_{\mathrm{Ks,x}}x_{\mathrm{s,x}}(\mathrm{V_{m,x}}\text{-}\mathrm{E_{Ks}})$$

$$g_{\mathrm{Ks,x}} = 0.057 + \frac{0.19}{1+e^{\text{-}(\log(\mathrm{Cai})+4.2)/0.6}}$$

$$\frac{dx_{\mathrm{s,x}}}{dt} = \frac{\bar{x}_{\mathrm{s,x}} - x_{\mathrm{s,x}}}{\tau_{\mathrm{s,x}}}$$

$$\bar{x}_{\mathrm{s,x}} = \frac{1}{1+e^{\text{-}(\mathrm{V_{m,x}}\text{-}1.5)/16.7}}$$

$$\tau_{\mathrm{s,x}} = \frac{1}{\dfrac{0.0719(\mathrm{V_{m,x}}+30)}{1\text{-}e^{\text{-}(\mathrm{V_{m,x}}+30)/6.76}} + \dfrac{0.131(\mathrm{V_{m,x}}+30)}{e^{(\mathrm{V_{m,x}}+30)/14.55}-1}}$$

$$E_{\mathrm{Ks,x}} = \frac{RT}{F}\frac{\left[\mathrm{K}^+\right]_\mathrm{o} + 0.0183\left[\mathrm{Na}^+\right]_\mathrm{o}}{\left[\mathrm{K}^+\right]_\mathrm{i} + 0.0183\left[\mathrm{Na}^+\right]_\mathrm{i}}$$

Plateau K^+ current, I_{Kp}

$$\mathrm{I_{Kp,x}} = g_{\mathrm{Kp,x}}k_{\mathrm{p,x}}(\mathrm{V_{m,x}}\text{-}\mathrm{E_{K,x}})$$

$$k_{\mathrm{p,x}} = \frac{1}{1+e^{\text{-}(\mathrm{V_{m,x}}\text{-}20)/5}}$$

Table 2. Physical constants

Parameter	Definition	Value
ρ_{ext}	Specific resistance of extracellular solution	83.33 Ω cm
C_{sc}	Specific capacitance of cellular membrane	0.01 pF μm^{-2}
R	Gas molar constant	8.310 J K^{-1} mol^{-1}
F	Faraday constant	96485 A s mol^{-1}
K	Absolute temperature	310 °K

Table 3. Geometric parameters of ventricular GP cell

Parameter	Definition	Value
L_c	Length of cell	130 μm
r_c	Radius of cell	5.93 μm
L_t	T-tubule length	5.93 μm
r_t	T-tubule radius	0.148 μm
$n_{t,\mu m}$	Number of T-tubules in 1 μm^2 of surface membrane	0.21 tubules μm^{-2}
$S_{m,s}$	Peripheral membrane area $(2\pi r_c^2+2\pi r_c L_c)$	5065 μm^2
$S_{m,t}$	Tubular membrane area $(4\pi^2 r_t L_t r_c L_c n_{t,})$	5609 μm^2
V_c	Volume of cell $(\pi r_c^2 L_c)$	1.436×10^{-5} μl
V_{myo}	Volume of myoplasm	0.778×10^{-5} μl
V_{NSR}	Volume of network SR	0.079×10^{-5} μl
V_{JSR}	Volume of junctional SR	0.0045×10^{-5} μl
V_{ss}	Volume of subspace	$0.586e\times10^{-9}$ μl

Table 4. L-type Ca^{2+} channel parameters

Parameter	Definition	Value
f	Transition rate into open state	300 s^{-1}
g	Transition rate out of open state	2000 s^{-1}
f'	Transition rate into open state for mode Ca	5 s^{-1}
g'	Transition rate out of open state for mode Ca	7000 s^{-1}
a	Mode transition parameter	2
b	Mode transition parameter	2
ω	Mode transition parameter	10 s^{-1}
$I_{Ca,half}$	I_{Ca} level that reduces $\overline{P}_k$ by half	-0.458 μA cm^{-2}

6. References

Amsellem, J. R., Delorme, C. Souchier, and C. Ojeda. 1995. Transverse-axial tubular system in guinea pig ventricular cardiomyocyte: 3D reconstruction, quantification and its possible role in K^+ accumulation-depletion phenomenon in single cells. *Biol. Cell* 85:43-54.

Brette, F., and C. Orchard. 2003. T-tubule function in mammalian cardiac myocytes. *Circ. Res.* 92:1182-1192.

Christé, G. 1999. Localization of K^+ channels in the T-tubules of cardiomyocytes as suggested by the parallel decay of membrane capacitance, IK_1 and IK_{ATP} during culture and by delayed IK_1 response to barium. *J. Mol. Cell. Cardiol.* 31:2207-2213.

Clark, R. B., A. Tremblay, P. Melnyk, B. G. Allen, W. R. Giles, and C. Fiset. 2001. T-tubule localization of the inward rectifier K^+ channel in mouse ventricular myocytes: a role in K^+ accumulation. *J. Physiol. (London)* 537.3:979-992.

Colatsky, T. J. 1980. Voltage clamp measurements of sodium channel properties in rabbit cardiac Purkinje fibres. *J. Physiol. (London)* 305:215-234.

Faber, G. M., and Y. Rudy. 2000. Action potential and contractility changes in $[Na^+]_i$ overloaded cardiac myocytes. A simulation study. *Biophys. J.* 78:2392-2404.

Findlay, I. 2002. Voltage-dependent inactivation of L-type Ca 2+ currents in guinea-pig ventricular myocytes. *J. Physiol. (London)* 545.2:389-397.

Frank, J. S., G. Mottino, D. Reid, R. S. Molday, and K. D. Philipson. 1992. Distribution of the Na^+-Ca^{2+} exchange protein in mammalian cardiac myocytes: an immunofluorescence and immunocolloidal gold-labeling study. *J. Cell Biol.* 117:337-345.

Grantham, C. J., and M. B. Cannell. 1996. Ca2+ influx during the cardiac action potential in guinea pig ventricular myocytes. *Circ. Res.* 79:194-200.

Hund, T. J., J. P. Kucera, N. F. Otani, and Y. Rudy. 2001. Ionic charge conservation and long-term steady-state in the Luo-Rudy dynamic cell model. *Biophys. J.* 81:3324-3331.

Iwata, Y., H. Hanada, M. Takahashi, and M. Shigekawa. 1994. Ca(2+)-ATPase distributes differently in cardiac sarcolemma than dihydropyridine receptor alpha 1 subunit and Na^+/Ca^{2+} exchanger. *FEBS Lett.* 355:65-68.

Jafri, M. S., J. J. Rice, and R. L. Winslow. 1998. Cardiac Ca^{2+} dynamics: the roles of ryanodine receptor adaptation and sarcoplasmic reticulum load. *Biophys. J.* 74:1149-1168.

Kieval, R. S., R. J. Bloch, G. E. Lindenmayer, A. Ambesi, and W. J. Lederer. 1992. Immunofluorescence localization of the Na-Ca exchanger in heart cells. *Am. J. Physiol.* 263:C545-C550.

Korchev, Y. E., Y. A. Negulyaev, C. R. W. Edwards, I. Vodyanoy, and M. J. Lab. 2000. Functional localization of single active ion channels on the surface of a living cell. *Nature Cell Biol.* 2:616-619.

Li, G. R., C. P. Lau, and A. Shrier. 2002. Heterogeneity of sodium current in atrial vs epicardial ventricular myocytes of adult guinea pig hearts. *J. Mol. Cell. Cardiol.* 34:1185-1194.

McDonough, A. A., Y. Zhang, V. Shin, and J. S. Frank. 1996. Subcellular distribution of sodium pump isoform subunits in mammalian cardiac myocytes. *Am. J. Physiol.* 270:C1221-C1227.

Nagatomo, T, Z. Fan, B. Ye, G. S. Tonkovich, C. T. January, J. W. Kyle, and J. C. Makielski. 1998. Temperature dependence of early and late currents in human cardiac wild-type and long Q-T DeltaKPQ Na+ channels. *Am. J. Physiol.* 275:H2016-H2024.

Noble, D., A. Varghese, P. Kohl, and P. Noble. 1998. Improved guinea-pig ventricular cell model incorporating a diadic space, IKr and IKs, and length- and tension-dependent processes. *Can. J. Cardiol.* 14:123-134.

Nordin, C. 1993. Computer model of membrane current and intracellular Ca^{2+} flux in the isolated guinea pig ventricular myocyte. *Am. J. Physiol.* 265:H2117-H2136.

Pásek, M., G. Christé, and J. Šimurda. 2001. Computer modelling of effect of transversal tubules on excitation - contraction coupling in cardiac cells (Basic study). in: *CD of the Conference Engineering Mechanics*, Svratka.

Pásek, M., G. Christé, and J. Šimurda. 2002. Quantitative modelling of effect of transverse-axial tubular system on electrical activity of cardiac cells: development of model. in: *CD of the Conference Engineering Mechanics*, Svratka.

Pásek, M., G. Christé, and J. Šimurda. 2003. Quantitative modelling of effect of transverse-axial tubular system on electrical activity of cardiac cells: development of model II. in: *CD of the Conference Engineering Mechanics*, Svratka.

Pásek, M., G. Christé, and J. Šimurda. 2004. Ionic concentration changes in the tubular system of rat ventricular cardiac cell model. in: *CD of the Conference Engineering Mechanics*, Svratka.

Rasmussen, H. B., M. Moller, H. G. Knaus, B. S. Jensen, S. P. Olesen, and N. K. Jorgensen. 2004. Subcellular localization of the delayed rectifier potassium channels KCNQ1 and ERG1 in the rat heart. *Am. J. Physiol.* 286:H11300-H1309.

Sakmann, B. F., A. J. Spindler, S. M. Bryant, K. W. Linz, and D. Noble. 2000. Distribution of a persistent sodium current across the ventricular wall in guinea pigs. *Circ. Res.* 87:910-914.

Sanguinetti, M. C., and Jurkiewicz, N. K. 1990. Two components of cardiac delayed rectifier K^+ current. Differential sensitivity to block by class III antiarrhythmic agents. *J. Gen. Physiol.* 96:195-215.

Scriven, D. R., P. Dan, and E. D. Moore. 2000. Distribution of proteins implicated in excitation-contraction coupling in rat ventricular myocytes. *Biophys. J.* 79:2682-2691.

Shepherd, N., and H. B. McDonough. 1998. Ionic diffusion in transverse tubules of cardiac ventricular myocytes. *Am. J. Physiol.* 275:H852-H860.

Taniguchi, A., J. Toyama, I. Kodama, T. Anno, M. Shirakawa, and S. Usui. 1994. Inhomogeneity of cellular activation time and Vmax in normal myocardial tissue under electrical field stimulation. *Am. J. Physiol.* 267:H694-H705.

Tourneur, Y., A. Marion, and P. Gautier. 1994. SR47063, a potent channel opener, activates KATP and a time-dependent current likely due to potassium accumulation. *J. Membr. Biol.* 142:337-347.

Wang, D. Y., S. W. Chae, Q. Y. Gong, and C. O. Lee. 1988. Role of aiNa in positive force-frequency staircase in guinea pig papillary muscle. *Am. J. Physiol.* 255:C798-C807.

Wang, Z., T. Mitsuiye, S. A. Rees, and A. Noma. 1997. Regulatory Volume Decrease of Cardiac Myocytes Induced by beta-Adrenergic Activation of the Cl^- Channel in Guinea Pig. *J. Gen. Physiol.* 110:73-82.

Yasui, K., T. Anno, K. Kamiya, M. R. Boyett, I. Kodama, and J. Toyama. 1993. Contribution of potassium accumulation in narrow extracellular spaces to the genesis of nicorandil-induced large inward tail current in guinea-pig ventricular cells. *Pflügers Archiv* 422:371-379.

Zeng, J., K. R. Laurita, D. S. Rosenbaum, Y. Rudy, K. Laurita, and D. Rosenbaum. 1995. Two components of the delayed rectifier K^+ current in ventricular myocytes of the guinea pig type. Theoretical formulation and their role in repolarization. *Circ. Res.* 77:140-152.